Three-Center−Two-Electron and Four-Center−Four-Electron Bonds. A Study by Electron Charge Density over the Structure of Methonium Cations

Nora B. Okulik,[†] Nélida M. Peruchena,[‡] and Alicia H. Jubert*[,§]

Facultad de Agroindustrias, UNNE, Cte. Fernández 755, (3700) Pcia. R. Sáenz Peña, Chaco, Argentina, Laboratorio de Estructura Molecular y Propiedades, Area de Quimica Fisica, Depto. Química, Fac. Ciencias Exactas, Nat. y Agrim., UNNE, Av. Libertador 5460, (3400) Corrientes, Argentina, and CEQUINOR, Centro de Química Inorgánica (CONICET, UNLP), Departamento de Química, Facultad de Ciencias Exactas, UNLP, C. C. 962, Facultad de Ingeniería, UNLP, 1 y 47, 1900 La Plata, Argentina

Received: June 14, 2006

We study the electronic density charge topology of CH_5^+ species **1** (C_s), **2** (C_s), and **3** (C_{2v}) at ab initio level using the theory of atoms in molecules developed by Bader. Despite the reports of previous studies concerning carbocationic species, the methane molecule is protonated at the carbon atom, which clearly shows its pentacoordination. In addition to the fact that hydrogen atoms in the methonium molecule behave in a very fluxional fashion and that the energy difference among the species **1**, **2**, and **3** are very low, is important to point out that two different topological situations can be defined on the basis of our study of the topology of the electronic charge density. Then, the species **1** and **2** present a three-center−two-electron (3c−2e) bond of singular characteristics as compared with other carbocationic species, but in the species **3**, the absence of a 3c−2e bond is noteworthy. This structure can be characterized through the three bond critical points found, corresponding to saddle points on the path bonds between the C−H(2,3,5) that lie in the same plane. These nuclei define a four-center interaction where the electronic delocalization produced among the σ(C−H) bonds provide a stabilization of the three C−H bonds involved in this interaction (the remaining two C−H bonds are similar to those belonging to the nonprotonated species). Our results show that bonding situations with a higher number of atom arrays are possible in protonated hydrocarbons.

Introduction

Toward the end of the last century and the beginning of this one, the current ideas in chemistry about the carbon tetravalency proposed by Kekulé (1850) and those about chemical bonding due to Lewis (1916), which can be considered as founding ideas of modern chemistry, are in intense evolution toward new perspectives that allow people to understand the mechanism of the catalytic reactions that take place in petrochemical processes[1] as well as the enzymatic reactions that happen in the nature.[2]

Recently Berkessel has proposed a catalytic mechanism for the dehydration of $CH_2{=}H_4MPT$ to $CH{=}H_4MPT^+$ and H_2 analogous to that elucidated by Olah for the reversible formation of carbocations and H_2 from alkanes in superacids.[3]

In this way, the idea of Lewis' chemical bond—as electronic pairs located between two united atoms—does not contemplate more complicated bonding situations such as those found in the chemistry of the carbocations, widely studied by Olah.[1]

The existence of protonated multicoordinated methanes (i.e., CH_5^+, CH_6^{2+}, and CH_7^{3+}) appear to extend the concept of the carbon tetravalency toward another more general situation in which the carbon atom would not be limited in its capability to bind to more than four atoms or groups.

An intense debate has been registered in the last years over the structure of CH_5^+, the prototype of nonclassical carbocations and hypercoordinated carbon species. Dramatic progress was achieved in the last few years, in terms of developing and applying novel atomistic computer simulation techniques. This was efficiently achieved due to an ingenious combination of electronic structure theory and molecular dynamics introduced by Car and Parrinello.[4]

New concepts and new ideas are the result of the continuous progress in the development of new computational tools, where the quantum mechanic methods, on the basis of more advanced sophisticated software, demonstrate a higher accuracy in the prediction of observable properties, allowing their application to more realistic and more complex situations. These developments led to new interpretations and in many cases the demand for revision and modification of established concepts.

In the chemistry of carbon, the carbonium ions are formed by the protonation of alkanes in superacid liquids [such as FSO_3H-SbF_5 (magic acid), $HF-SbF_5$ (fluoroantimonic acid), triflic acid systems]. Furthermore, some solid superacids (such as certain zeolites and other supported systems) are being of substantial practical, even industrial, use.

The high acidity of the catalysts and high temperature compensate for the well-known inertness of the starting material. It is widely accepted that the reactions proceed via an ionic mechanism.[5] The initial step is, however, often ascribed[6] as a proton attack on C−C or a C−H bond, following the concept of σ-reactivity developed by Olah and his group in the framework of extensive investigation of electrophilic reactions of single bonds in superacid media.[7,8]

While these species have a too short lifetime to allow direct observation in superacid media by NMR, hydrogen exchange and cleavage reactions have been described elsewhere.[9]

* Corresponding author. E-mail: jubert@quimica.unlp.edu.ar.
[†] Facultad de Agroindustrias, UNNE.
[‡] Laboratorio de Estructura Molecular y Propiedades, UNNE.
[§] CEQUINOR, UNLP.

10.1021/jp063709m CCC: $33.50
Published on Web 07/26/2006

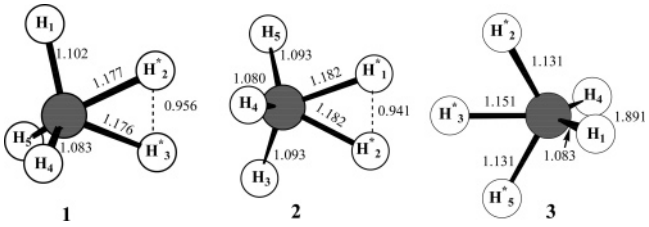

Figure 1. Optimized geometries of species **1**, **2**, and **3** of CH_5^+ ion. Calculated at the MP2(full)/6-31G** level.

Small alkonium ions, such as CH_5^+ and $C_2H_7^+$, have been originally detected in high-pressure mass spectrometry experiments[10,11,12] and later on they have been studied on a quantitative basis. The first reference to the three-center−two-electron (3c−2e) bond in CH_5^+ was by Dyczmons,[13] who interpreted its character on the basis of Boys' localization, while Muller et al. stated[14] when considering the C_{2v} structure of the CH_5^+ ion "in the C_{2v} structure the proton interacts equally with two CH bonds, such that a 5-center 4-electron bond is formed" (the two orthogonal hybrid atomic orbitals (AOs) of carbon atom are considered as two centers).

Although numerous experimental studies have been performed on the CH_5^+ ion[11,12,15] and $C_2H_7^+$ ion,[19,20] it was not until 1999 that Oka and his collaborators succeeded in obtaining the high-resolution IR spectrum of the CH_5^+.[16] During the last years it was not possible to carry out a detailed assignment of the individual lines, due to the complexity of the obtained spectrum, and the results seem to confirm theoretical predictions that this molecule is highly fluxional and that the term "structure" should have to be refined.[14,17,18] Recently, the infrared spectrum of bare CH_5^+ was presented by Asvany et al.[21] Their measurements together with ab initio molecular dynamical calculations provide a mechanism for exchange of hydrogens between CH_3 tripod positions and the three-center bonded H_2 moiety that eventually leads to full hydrogen scambling. More recently, the quantum deconstruction of the infrared spectrum of CH_5^+ was published by Huang et al.[22]

The interest in the CH_5^+ cation led to numerous studies, mainly for the apparent difficulty in locating structures of minimum energy of well-defined geometry. Nevertheless, different structures for the methonium cation were proposed theoretically[23] (see also references therein) (Figure 1). The energetics of these systems has been studied rigorously in the frame of the most sophisticated theory levels.[14,17,18,24−29] A full-dimensional, ab initio based potential energy surface (PES) for CH_5^+, which can describe dissociation, is reported in ref 23.

The protonated methane possesses a surface of potential energy that involves about 120 identical minima, each one involving a structure with a 3c−2e bond in the CH_2 group, and they can interconvert with a very low amount of energy. Considering the minimum as the reference energy (eclipsed C_s (**1**)), the energies of the staggered C_s (**2**) and C_{2v} (**3**) saddle points on the PES are 29.1 and 340.7 cm^{-1}, respectively.[24]

Calculations carried out within the Born−Oppenheimer approach, where it is assumed that the positions of the nuclei will not suffer large changes in the minimum of the PES, have shown that, although the species **1** of eclipsed C_s symmetry (Figure 1) represents the most stable structure of CH_5^+ (a global minimum), the two other low-energy stationary points on the PES, species **2** and **3**, are practically isoenergetic to species **1**. The staggered C_s (**2**) corresponds to a first-order saddle point for the rotation of the H_2 moiety around the pseudo-C_3-axis of the tripod [C_s (**1**) → C_s (**2**) → C_s (**1**)] and species **3** corresponds to a C_{2v} saddle-point structure (without H_2 moiety) for the scrambling of the hydrogens.

Several authors[14,17,18,24] suggested that the CH_5^+ cation does not have a defined structure, since the protons are extremely mobile and, therefore, the representation with a 3c−2e bond, present in C_s structures, is an oversimplification.

Beyond of the static study of CH_5^+, Marx and Parrinello performed different types of ab initio molecular dynamics calculations,[27,29] for example, ab initio path integral molecular dynamics calculations, in which the nuclear vibrational and electronic wave functions were calculated simultaneously, and standard Car−Parrinello molecular dynamics calculations,[4] in which the nuclei were treated classically.[29b] Of these works one concludes that CH_5^+ is a fluxional molecule that undergoes hydrogen scrambling and pseudorotations. According to Marx and Parrinello,[27] the quantum ground state is dominated by configurations in which the moiety H_2 is united to tripod CH_3^+, C_s configurations, with a 3c−2e bond, as had been suggested by Olah and his collaborators in 1969,[9] based on the fact that H_2 is formed by the reaction of methane with liquid superacid media. However, Marx and Parinello[27] have not detected a full scrambling of hydrogen, probably because the time of running considered in the dynamics could have been very short. An observation that soon was confirmed by the work of Thompson.[30]

Thompson used the quantum diffusion Monte Carlo method (QDMC) in order to calculate the nuclear vibrational wave function and zero-point energy of CH_5^+ and its rotational constants over an interpolated potential energy surface from CCSD(T)/aug′-cc-pVTZ ab initio data. Due to the calculations, Thompson found that CH_5^+ rather than remaining localized in a single energy minimum on the PES can only be described by a nuclear vibrational wave function that accesses large areas of conformational space. All five hydrogen atoms in CH_5^+ possess identical C−H and H−H radial distribution functions within the nuclear vibrational wave function and are quantum mechanically equivalent. In these simulations, direct calculation on the potential energy is not performed at the light level of ab initio theory because of the number of potential energy evaluations required. The ground-state CH_5^+ wave function has some C_s (**1**) character, as evidenced by the bimodal character of the H−H radial distribution function; however, there is considerable delocalization of the protons, and the calculated rotational constants (very similar among them) suggesting that the CH_5^+ ground-state structure is more symmetric than the C_s (**1**) global minimum energy configuration. Thompson's conclusion was that "CH_5^+ is indeed a fluxional molecule".

According to these authors there is a substantial proton scrambling, even at 0 K. On the other hand, Brown et al.[31] have analyzed the degree of localization of the wave function in order to establish what fraction of the amplitude is located in each of the 120 equivalent minima. Comparative results from diffusion Monte Carlo (DMC) ground state, harmonic ground state, and molecular dynamics simulation are showed in ref 31. In the context of the harmonic description, the ground-state wave function has 75% of this amplitude in the minimum around which it is expanded and more than 99% of the amplitude is distributed over the three minima that are connected to it through the C_s (**2**) and C_{2v} (**3**) saddle points.

In conclusion, there is substantial amplitude in the C_s (**1**) equivalent minima but also comparable amplitude at the C_s (**2**) and C_{2v} (**3**) saddle points that connect these minima.

Recently, a full-dimensional MP2/cc-pVTZ PES has been constructed by McCoy and co-workers[32,33] (by fitting 20 633

ab initio data points to a polynomial expansion in the symmetry coordinates for CH_5^+ using 2303 coefficients). This PES was used in ab initio DMC calculations of the fully anharmonic zero-point energies and ground-state wave functions of CH_5^+ and $CH_2D_3^+$. In this paper, bond length distributions are obtained from the DMC ground state and are compared to those resulting from classical molecular dynamics simulations, which are performed at the quantum zero-point energy for roughly 300 ps. They report that, because the zero-point energy is still much larger than the barriers between the minima, the classical trajectory is run at the zero-point energy samples at all the 120 potential minima, which have equal probability. As a result, the distributions of the distances are nearly identical to the corresponding *r*CH or *r*HH distributions for CH_5^+. In contrast, the distributions that are based on the DMC ground state deviate substantially from the corresponding picture for CH_5^+.

According to McCoy and his collaborators, even in the classical description, the propensity of the hydrogen atoms in CH_5^+ to partition into one group that forms a H_2 unit and another group that forms a CH_3^+ unit can be clearly seen.

Kumar and Marx,[34] in a recent study involving ab initio molecular dynamics simulations at different temperatures, compared computed infrared spectra to the measured one, giving support to the high fluxionality of CH_5^+. Considering the analysis of the trajectories of the dynamic simulation at 300 K and taking the criterion of 1.15 Å as the maximum allowed distance between a pair of protons to be considered as a H_2 moiety, they suggest that "little over 80% of its configurations correspond to C_s-like structure" (compared to 100% at 50 K), which is close to the previous estimate extracted from low-temperature ab initio path integral quantum simulations.[27] This analysis has shown "why bare CH_5^+ can be characterized to a large extent, though not entirely, by C_s-like ground-state structures." On the other hand, the fact that C−H stretching modes involving the carbon nucleus and those protons that form the H_2 moiety and the CH_3 tripod, respectively, result in distinct peaks is an experimental support for three-center−two-electron bonding being present in experimental conditions. According to Kumar et al., the peculiar dynamic of CH_5^+ might be represented by "correlated motion" of the five protons around the central carbon nucleus.

In general, calculations show that the CH_5^+ cation undergoes rotation of the H_2 moiety and scrambling of the hydrogens (or, as Olah denominates, "bond-to-bond rearrangements"). To arrive at a comprehensive understanding of CH_5^+, cutting-edge experimental and theoretical studies will be needed.[29]

Regarding this question, the topological calculations on species of CH_5^+ (Figure 1) can be very interesting. The topology of a molecular charge distribution yields a single unified theory of molecular structure, one that defines atoms, bonds, structure, and the mechanisms of structural change. In this theory one may unambiguously assign a *chemical structure* to a molecule by determining the number and kind of critical points (CPs) in its electronic charge distribution. Application of the theory of atoms in molecules[35] (AIM) to understand the nature of the 3c−2e bonds in carbonium ions in deeper detail has been performed by our group for other carbonium ion structures.[36] A deep knowledge of the electronic structure of the carbocationic species is essential in order to understand the mechanisms that occur during the catalytic process in the transformation of hydrocarbons.

Previusly, Savin et al.[37] used the function of electronic localization ELF in representative configurations of CH_5^+ (considering a set of configurations obtained from ab initio quantum simulations from Marx et al.[27]) to show the hierarchical bifurcation analysis in C_s-like and C_{2v}-like configurations.

The associated bifurcation diagrams in both configurations are topologically different. In the first, are defined four basins, one of them associated with the bonding electron pair of the H_2 moiety bonding to the carbon nucleus and the other three basins associated with standard C−H two-center−two-electron (2c−2e) bonds. The second diagram show three basins: one of them contains 4e and the other two basins have 2e each.

Finally, such analysis suggests that CH_5^+ is indeed very floppy but shows considerable preference for C_s-like structures.

In this work, the topology of the electronic density charge is studied for CH_5^+ species at ab initio level using AIM developed by Bader.[35] In our work, we are allowed to localize the bond critical points along the bond path moving through the density maxima and we also can obtain the molecular graphs for the C_s species (**1** and **2**) and the transition state C_{2v} (species **3**) of the methonium ion.

In a complementary form to the information provided by ELF analysis and contrary to Savin's work, we can determine for each configuration which atoms are bonded among them by a bond path and contribute to the understanding of the hydrogen scrambling based on the topological properties of the charge density in bond critical points (BCPs) in multicenter bonds.

The electronic delocalization that operates through the σ-bonds in saturated molecules and specifically in protonated alkanes can be studied by means of analysis of the charge density and the BCPs. This analysis will be used in order to establish the features of the multicenter bonds in the different species **1**, **2**, and **3** in CH_5^+ cation and to be able to relate them with the proposed structures of the methonium ion and also in order to understand their high fluxionality.

From the analysis of the electronic density and the bond paths it arises that the carbon atom is pentacoordinated and that no bonding critical point is found between any pairs of hydrogen atoms. We discuss the relative stability of the 3c−2e vs 2c−2e bonds in C_s-like species (**1** and **2**) and relate this fact to hydrogen scrambling in CH_5^+ and also characterize the four-center−four-electron (4c−4e) bond in the transition state for scrambling of hydrogen in C_{2v}-like species (**3**).

Recently, Tantillo and Hoffmann[38] claim the discovery of the system containing five-center−four-electron bonding localized in the central (C···H···C···H···C) fragment of a cation. It is probable that the existence of nonclassical bonds involving more than three centers, with different bonding parents, cannot be completely excluded in the carbocation chemistry. The eventual existence of such bonds thus still represents an interesting challenge for the theoretical chemistry.

Method and Calculation Details. Calculations at the Hartree−Fock single-reference second-order Moller−Plesset perturbation theory (MP2) were performed for methane and methonium cations (Figure 1). The geometries of all the species were fully optimized. The nature of all stationary points was characterized by calculation of the Hessian matrix and analyzing the normal vibrational modes. The structure **1** was confirmed as a true minimum over the potential energy surface by the presence of real harmonic frequencies, and the structures **2** and **3** were characterized as first-order saddle point by the presence of only one imaginary harmonic vibrational frequency.

Calculations were carried out at the MP2(full)/6-31G** level without any restrictions. The calculations were performed using the Gaussian98 package.[39]

The topological analysis and the evaluation of the local properties were carried out with the program PROAIM[40] using

TABLE 1: Topological Properties (in au) of the Electronic Charge Density in the BCP of Structures 1, 2, and 3 of Methonium Ion[a–c]

structure	bond[d]	ρ_b	$^2\rho_b$	λ_1	λ_2	λ_3	$\lvert\lambda_1\rvert/\lambda_3$	e	G_b/ρ_b	$\lvert V_b\rvert/G_b$	E_b
	C−H*$_2$	0.2251	−0.5468	−0.4993	−0.1637	0.1163	4.2930	2.0495	0.2687	4.2595	−0.1972
1	C−H*$_3$	0.2198	−0.5065	−0.5309	−0.1448	0.1691	3.1396	2.6674	0.2502	4.3018	−0.1816
	C−H$_1$	0.2685	−0.9491	−0.7178	−0.6981	0.4668	1.5377	0.0281	0.1255	9.0386	−0.2709
	C−H$_4$	0.2895	−1.1011	−0.8223	−0.7979	0.5190	1.5844	0.0305	0.0953	11.9710	−0.3028
	C−H$_5$	0.2895	−1.1011	−0.8223	−0.7979	0.5190	1.5844	0.0305	0.0953	11.9710	−0.3028
	C−H*$_1$	0.2225	−0.5295	−0.5086	−0.1008	0.0799	6.3654	4.0464	0.2526	4.3559	−0.1886
2	C−H*$_2$	0.2225	−0.5249	−0.5088	−0.1009	0.0802	6.3441	4.0422	0.2526	4.3559	−0.1886
	C−H$_3$	0.2776	−1.0193	−0.7703	−0.7435	0.4945	1.5577	0.0360	0.1099	10.3574	−0.2854
	C−H$_4$	0.2944	−1.1335	−0.8376	−0.8215	0.5257	1.5933	0.0195	0.0896	12.7348	−0.3098
	C−H$_5$	0.2776	−1.0190	−0.7700	−0.7433	0.4943	1.5577	0.0359	0.1101	10.3336	−0.2853
	C−H$_1$	0.2875	−1.0865	−0.08159	−0.7892	0.5186	1.5733	0.0339	0.0973	11.7084	−0.2996
3	C−H$_4$	0.2875	−1.0865	−0.08159	−0.7892	0.5186	1.5733	0.0339	0.0973	11.7084	−0.2996
	C−H*$_3$	0.2149	−0.4948	−0.5609	−0.2725	0.3386	1.6565	1.0581	0.2959	3.9465	−0.1874
	C−H*$_2$	0.2430	−0.7348	−0.6080	−0.4971	0.3703	1.6419	0.2230	0.1831	6.1258	−0.2281
	C−H*$_5$	0.2430	−0.7346	−0.6079	−0.4970	0.3702	1.6421	0.2232	0.1830	6.1300	−0.2281

[a] See Figure 1 and text for the explanation of symbols. [b] ρ_b, $^2\rho_b$, λ_i, G_b/ρ_b, and E_b in au. [c] Topological properties in BCP of C−H bonds in methane: $\rho_b = 0.2813$au, $\nabla\rho_b = -1.0106$ au, $\lambda_1 = -0.7029$ au, $\lambda_2 = -0.7029$ au, $\lambda_3 = 0.3951$ au, $|\lambda_1|/\lambda_3 = 1.7790$, $\epsilon = 0.0000$, $G_b/\rho_b = 0.1578$ au, $|V_b|/G_b = 7.6892$, $E_b = -0.2970$ au. [d] An asterisk indicates atoms involved in a multicenter bond.

the wave functions obtained at MP2(full)/6-311++G** level with the Gaussian98 program.[39]

Results

Methonium Ion (CH_5^+) Species 1 and 2. The optimized geometry of the CH_5^+ cations, structures **1** (C_s), **2** (C_s), and **3** (C_{2v}), is shown in Figure 1, together with the most relevant geometric parameters calculated at MP2(full)/6-31G** level, expressed in au.

In structure **1**, the 3c−2e bond in the CH*$_2$ group is located in a plane with the C−H bond, denoted C−H$_1$. The CH*$_2$ is eclipsed with the C−H bonds of the CH_3 moiety. The methane molecule has been distorted by the protonation (C−H bond (1.084 Å)). Considerably larger C−H* bonds (1.177 Å) and an angle H*$_2$−C−H*$_3$ of 48° result. The hydrogen atom that is coplanar with the C−H* bonds presents a bond length of 1.102 Å and it forms an angle H$_1$−C−H* of 75.8°. The other two bonds practically do not change (1.083 Å with an angle H−C−H of 119.5°).

Table 1 shows the most significant topological local properties at the bond critical points in methonium cations, structures **1**, **2**, and **3**.

The topological properties at the BCPs of the C−H bonds in methane and in the CH_5^+ ion are similar and characteristic of shared interactions—covalent bonds—and they have large ρ_b values, $\nabla^2\rho_b < 0$, $|\lambda_1|/\lambda_3 > 1$, $G_b/\rho_b < 1$ (G_b being the local kinetic energy density at the bond critical point) and considerable negative values of the local total energy density, E_b.

The comparative analysis on the BCP of the C−H*$_{2,3}$ vs C−H$_{1,4,5}$ bonds in species **1** allows us to make the following comments: In the C−H* bonds a lower concentration of the electronic charge density (of 0.29−0.22 au) can be seen between the carbon atom and the hydrogen atoms, involving in the 3c−2e bond, denoted H*, with respect to other C−H bonds. This decrease in ρ between both atoms that form the bond is caused by the decrease in the perpendicular contractions of the density toward the path bond in both directions perpendicular to the trajectory of the bond. This diminution of the contraction of the density is higher in the direction of eigenvector associated with eigenvalue λ_2.

On the other hand, it is evident that the diminution of the density at BCP is not due to an increase on the expansion of the ρ_b toward the path bond (associated with eigenvalue λ_3). It can be observed in Table 1 that λ_3 does not increase but drops its value, evidence of the dominance of the contraction over the expansion of the density in the analyzed interactions.

Accompanying the lower ρ_b values, less negative $\nabla^2\rho_b$ values are observed in C−H* bonds (with respect to methane and to other C−H in methonium). One should keep in mind that the Laplacian magnifies the small changes in the electron density upon bond formation. The Laplacian values in these bonds decrease to half of their current values ($\nabla^2\rho_b = -1.1011$ au in C−H and −0.5468 and −0.5065 au in the other two C−H*$_{2,3}$ bonds, respectively). Also, the relationship between the perpendicular and parallel curvature at BCP, $|\lambda_1|/\lambda_3$, is notably higher (2.7 times higher) in the C−H*$_{2,3}$ bonds than in the C−H ones. Regarding the energy densities, at BCP, it can be seen that the potential energy density values, V_b, are slightly lower. Notwithstanding, the kinetic energy density values, G_b, in the C−H*$_{2,3}$ bonds are remarkably greater than those on the C−H in species **1** and in methane taken as reference. As a consequence of what was pointed out above, dramatic differences in kinetic energy density per charge unit, G_b/ρ_b, and in the relationship $|V_b|/G_b$ are found. Thus, G_b/ρ_b, is 2.8 times higher, whereas $|V_b|/G_b$ is three times smaller for the C−H* than for the C−H ones, although local topological property values in such BCPs agree with usual values of a shared interaction.

A dramatic change in the ellipticity value can be also observed in Table 1 (from 0.030 in the C−H$_{4,5}$ bond in **1**, to 2.049 and 2.667 for the C−H*$_{2,3}$ bonds in species **1**). The abnormally high ellipticity value, at C−H* BCP for the species **1**, as well as the high value of the $|\lambda_1|/\lambda_3$ relationship, indicate that the (3, −1) BCPs are less stable that the other bonds. This increase of the ellipticity is related to the instability of the bond: this is a bond with high ellipticity ($\epsilon \gg 1$)—caused by an abrupt diminution of λ_2—that is always related to the proximity of a structural change, possibly a pseudorotational rearrangement of the species **1**.

As mentioned above, the eigenvectors associates with the eigenvalue λ_3 defines a unique pair of trajectories of gradient ρ that originate at BCP, each of which terminates at a nucleus of one the neighboring atoms. This pair of trajectories defines a line through space along which the electron density is a maximum with respect to any neighboring line designed as an atomic interaction line or bond path. Each bond path is homeomorphically mirrored by a virial path, a line of maximally negative potential energy density linking the same nuclei. Thus,

the presence of a bond path and its associated virial path provide a universal indicator of bonding between the atoms so linked.[35]

The Laplacian of ρ also appears in the local expression of the virial theorem, which can be written as

$$h^2/4m\ \nabla^2\rho = 2\ G(r) + V(r)$$

Since $G(r) > 0$ and $V(r) < 0$, the lowering of the potential energy dominates the total energy in those regions of space where electronic charge is concentrated, where $\nabla^2\rho_b < 0$, while the kinetic energy is dominant in regions where $\nabla^2\rho_b > 0$.

In a shared interaction, electron density is both accumulated and concentrated along the bond path between the nuclei, and this can be seen in all C−H bonds in methonium. However, it is important to highlight that the degree of accumulation of the charge density in the BCPs corresponding to $C-H^*_{2,3}$ bonds in **1** and $C-H^*_{1,2}$ bonds in **2** (measured by the value for ρ_b), and the extent of concentration of the density (measured by the magnitude of $\nabla^2\rho_b$) are diminished at these bonds.

On the other hand, the density of the total electronic energy function is related to the density of the potential and kinetic energy by the expression

$$E_e(r) = G(r) + V(r)$$

where $E_e(r)$ designs the density of the local total electronic energy.

As can be seen in Table 1, lower magnitudes of $-E_b$ are found in the BCPs corresponding to the $C-H^*_{2,3}$ in **1** and $C-H^*_{1,2}$ in **2**, due to a slight diminution of the potential energy and a marked increase of the kinetic energy. However, in the five BCPs corresponding to the C−H bonds the potential energy is dominant, $\nabla^2\rho_b < 0$ and $E_e < 0$ as a result of the contraction of the density along the line of interaction.

Figure 2a shows the contour maps of the Laplacian distribution $\nabla^2\rho(r)$ for the methane in the plane that contains the carbon atom and the two hydrogen atoms. The molecular graph, defined by the network of trajectory of the bond or bond paths, in the plane selected is superimposed. In this figure the BCPs are indicated with circles. The projection over the plane of the remaining two C−H bonds underlying the plane that bisects the previous one can also be observed. In this map regions of concentration ($\nabla^2\rho(r) < 0$) and depletion ($\nabla^2\rho(r) > 0$) of the electronic charge density, indicated by dotted contour lines and full lines, respectively, can be seen.

Due to the symmetry of CH_4, the topological properties in the BCPs and the contour map of the Laplacian distribution in different planes are identical (they are not shown due to this reason). The topological properties corresponding to the four C−H bonds in methane are shown at the bottom of Table 1.

Figure 2b shows the contour map of the Laplacian distribution $\nabla^2\rho$ and the molecular graph for the methonium cation, **1**, in the plane that contains the carbon and the three hydrogen atoms, the two hydrogen atoms of the 3c−2e bond, and the hydrogen atom H_1. The relatively small bond angle H*−C−H* in CH_5^+ leads to a concentration of the electronic charge density involving the three atoms, giving a three-center−two-electron bond of H*−C−H* type, which is well-characterized by the topology of $\nabla^2\rho(r)$. The curved path bonds corresponding to these C−H* bonds show higher values of the ellipticity and lower values of local potential and total electronic energy densities, both evaluated at BCP.

Figure 2c shows, in a perpendicular plane to the previous one, the other pairs of $C-H_{4,5}$ bonds. The similarity with the corresponding map of the nonprotonated species (Figure 2a) and its difference with that in Figure 2b can be seen.

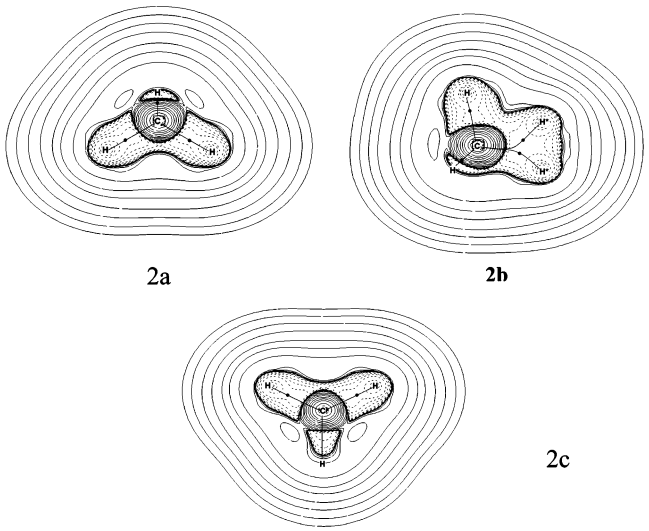

Figure 2. Contour maps of the Laplacian distribution $\nabla^2\rho(r)$ and molecular graphs for (a) the methane in the plane that contains the carbon atom and the two hydrogen atoms; (b) the methonium cation **1**, in the plane that contains the carbon and the hydrogen atoms of the 3c−2e bond; (c) the pairs $C-H_{4,5}$ bonds in a plane perpendicular to the previous one. Lines connecting the nuclei are the bond paths and the small dots along them represent the bond critical point (BCP). Solid lines represent regions of electronic charge concentration, and broken lines denote regions of electronic charge depletion. The contours of the $\nabla^2\rho(r)$ increase (+)/decrease (−), respectively, from the zero contour in the order $\pm 2 \times 10^{-n}$, $\pm 4 \times 10^{-n}$, $\pm 8 \times 10^{-n}$, with n beginning at 3 and decreasing in steps of unity. The same set of contours is used in all the figures of this work. The molecular graphs are superimposed. Note (in Figure 2b) the two long and curved bond paths corresponding to $C-H^*_{2,3}$.

This figure and the values of the Laplacian for these bonds (see Table 1) allow one to distinguish differences between the C−H* bonds involved in the three center−two electron bond, where the Laplacian has taken lower values than the remaining C−H bond. However, all the C−H bonds can be characterized as shared interactions, with accumulation of the electronic density between the nuclei.

This figure also shows the molecular graph of the methonium, where the BCPs are shown. It can be observed that the 3c−2e bond presents two critical points; its bond paths are indicative of two C−H* bonds and the missing of the bond path (and the BCP) binding both hydrogen atoms. Thus, the existence of this interaction line between two atoms is necessary and a sufficient condition of a chemical bond. This situation is not observed among the H* atom, so it allows us to state that, at least from a topological point of view, the carbon atom in the CH_5^+ ion is really directly bound to five hydrogen atoms. From the topological point of the view, the distribution of the density of the methonium is exceptional and not a model of a series. It is necessary to highlight that this situation is unique among all the carbocations previously studied by our group.[36] In the case of the 1-H and 2-H ethonium, proponium, and butonium cations, the 3c−2e bonds involve bonds of the type C−H* and H*−H*; it is a long and curved bond path that is found between carbon and hydrogen asterisk atoms and another path bond is found between both hydrogen atoms, indicated with an asterisk.

The topological distribution of the density of the cation **2** shows similarities and differences regarding the species **1**. The CH_2 fragment that corresponds to the three-center bond is formed between $H^*_1-C-H^*_2$ (the bond angle is 46.9°). The

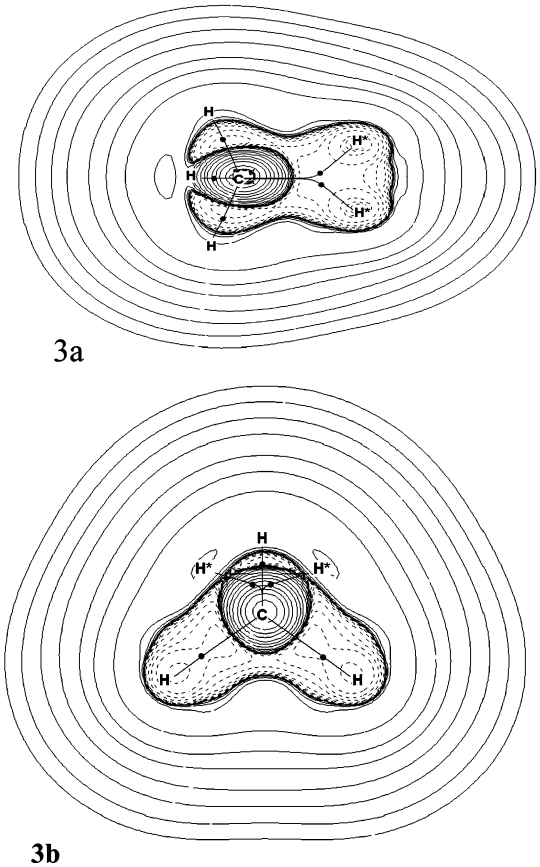

Figure 3. The contour maps of the Laplacian $\nabla^2\rho$ in species CH_5^+ **2** are shown (a) in the plane that contains the 3c−2e bond and (b) in the plane perpendicular to the previous one. The molecular graphs are superimposed. Lines connecting the nuclei are the bond paths and the small dots along them represent the bond critical point (BCP). Solid lines represent regions of electronic charge concentration, and broken lines denote regions of electronic charge depletion. The same set of contours is used in all the figures of this work.

fragment CH^*_2 is found in a staggered configuration regarding the other hydrogen atoms of the CH_3 fragment. As in the species **1**, the C−H* bonds that participate in the three-center bond are energetically less stable that the other $C-H_{4,5,3}$, bonds. However, in **2** the ellipticity values for these bonds increase significantly ($\epsilon = 4.04$ and 4.05 vs 2.05 and 2.67).

The other two $C-H_{3,5}$ bonds are similar to the C−H bonds in the methane molecule, as mentioned above in the species **1**. Notwithstanding, the fifth bond, (i.e. the $C-H_4$) has the highest density and Laplacian values and the lowest ellipticity of all values, with a slight increase in the density of the kinetic energy per charge unity. This is the bond that proves to be the most stable ($E_b = -0.3098$ au and $\epsilon = 0.019$) of the five C−H bonds in species **2**.

The contour maps of the Laplacian $\nabla^2\rho$ in species **2** are shown in Figure 3a,b in two perpendicular planes. Figure 3a shows the three-center bond (that lie in the plane of the figure) and the projection of the other three that are found out of the plane. Note the absence of the bond path that connects both hydrogen atoms, in agreement with what was explained previously. Figure 3b shows the two $C-H_{3,5}$ bonds that lie in the plane and the other three bonds that are out of this plane. Note the similarity with Figure 2c of the species **1** and with Figure 2a corresponding to the two C−H bonds in the methane molecule.

In summary, the increment in the ellipticity value in the BCP in the 3c−2e bonds in the species **1** and **2** is correlated with an abrupt decrease in the perpendicular curvature λ_2. Also, a marked decrease in the parallel curvature λ_3 can be observed. As a consequence of this last behavior, higher values for the density of the kinetic energy per charge unity are registered, G_b/ρ_b. The relationship between the densities of the potential and kinetic energies ($|V_b|/G_b$) decreases to less than a half, due to the increase in G_b, which duplicates its value in the three-center bond, and a slight decrease in $|V_b|$. These values of the energy density lead to a lower value of the density of the electronic energy ($-E_b = 0.18-0.19$ au), showing the destabilization of the 3c−2e bond against the remaining C−H bonds in this species of CH_5^+ cation.

As was pointed in previous papers related to Bader's theory, the interatomic interactions arise from a balance between kinetic and potential energy or, in other words, from a balance between the concentration of the charge density (perpendicular contractions) along the bond path between the nuclei linked and the parallel expansion of ρ, with density being concentrated separately in each atomic basin. If the Laplacian is negative, the contraction along the trajectory of the bond will show a local gain in the potential energy due to the increase of the charge density that is shared by both atoms. This can be observed in all cases, but in the BCPs corresponding to $C-H^*_{2,3}$ in **1** and $C-H^*_{1,2}$ in **2**, the value of the Laplacian is reduced to half. That is, the local gain of the potential energy in the BCPs corresponding to the bonds involved in the 3c−2e bonds is less that in the BCPs corresponding to the others C−H's and the $-E_b$ is also lower.

Considering that every bond path (a line through space along which the electron density is a maximum with respect to any neighboring line) is mirrored by a virial path, a line linking some neighboring nuclei, along which the potential energy density is maximally negative, i.e., maximally stabilizing, with respect to any neighboring line, the relative stability of the C−H bonds vs the C−H* bonds can be established with respect to the relationship between potential and kinetic energy. As $|V_b|/G_b \gg 1$ in all C−H bonds (see Table 1), corresponding to shared interactions, the diminution of this relation is indicative of the reduction of the stability in these interactions.

In other words, the shared interactions achieve their stability through the lowering of the potential energy resulting from the accumulation of electronic charge between the nuclei, then the diminution of concentration and accumulation of the density between the carbon and H* atoms are indicative of the lower stabilizations in this bonds.

Species 3. The contour maps of the Laplacian $\nabla^2\rho$ in species CH_5^+ **3** are shown in Figure 4a,b. In the cationic species **3** (C_{2v}) several important differences regarding the previous two species can be seen. Two fragments can be defined, CH_2 and CH_3, but no 3c−2e bonds are observed. However, an electron-defficient region established against the C atom and the three Hydrogen atoms ($H^*_{3,2,5}$) that lie in the same plane can be described. This interaction, called "four centers", defines a net of bond trajectories (localized in a plane perpendicular to that containing the other two remaining bonds; see Figure 4a) that present interesting topological properties: the three BCPs of the 4c−4e bonds show $-E_b$ values indicative of stabilized bonds, and the ellipticity values are much smaller that those found in the 3c−2e bonds of the remaining carbocationic species.

In this species, very different values of ellipticity can be observed in the BCPs ($\epsilon_{1,4} = 0.0339$ for the two C−H that do not participate in the four-center bond; $\epsilon_{2,5} = 0.2230$ for the other pair of C−H and $\epsilon_3 = 1.0581$ for the $C-H_3$ that is found in the same plane out of the two previous ones, bisecting the

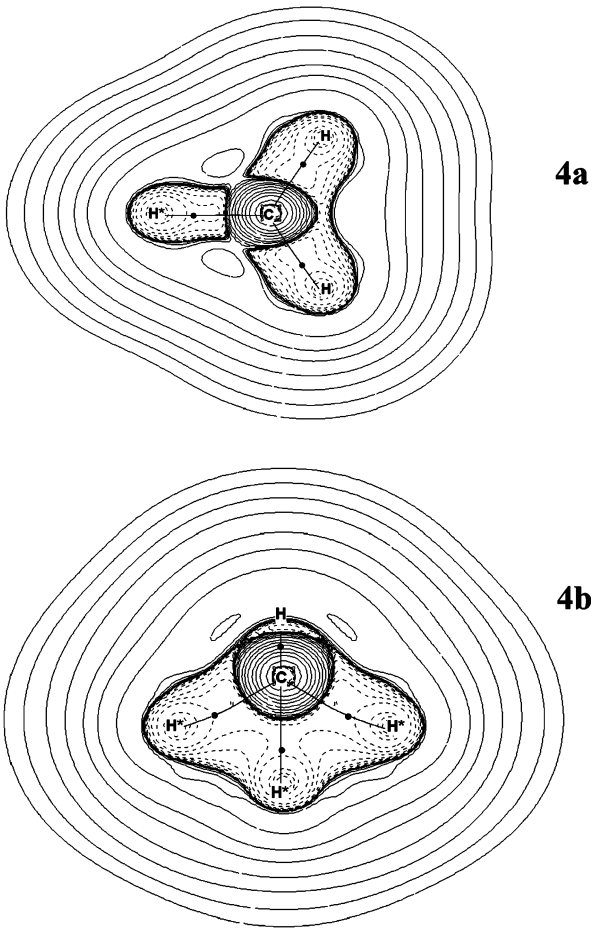

Figure 4. The contour maps of the Laplacian $\nabla^2\rho$ in species CH_5^+ **3** are shown (a) in the plane that contains the four-center interaction, $C-H^*_{2,3,5}$ and (b) in the plane perpendicular to the previous one. The molecular graphs are superimposed. Lines connecting the nuclei are the bond paths, and the small dots along them represent the bond critical point (BCP). Solid lines represent regions of electronic charge concentration, and broken lines denote regions of electronic charge depletion. The same set of contours is used in all the figures of this work.

first two). The map in Figure 4b shows the plane defined by the C atom and the two $H_{1,4}$ atoms very similar to that of the C−H bond belonging to the methane molecule.

The values of ρ_b and $\nabla^2\rho_b$ decrease in the order $C-H_{(1,4)} > C-H^*_{(2,5)} > C-H^*_{(3)}$, while the ellipticity values increase in the order $C-H_{(1,4)} < C-H^*_{(2,5)} \ll C-H^*_{(3)}$, respectively. The increase in the ellipticity values corresponds with the decrease in the values of density of the electronic energy ($-E_b$). Thus, the stability of these bonds (according to $-E_b$ values) decreases in the following order: $C-H_{(1,4)} > C-H^*_{(2,5)} > C-H^*_{(3)}$. To distinguish what is observed in **1** (C_s) and **2** (C_s), the values of the curvatures λ_2 and λ_3 do not show a decrease in the CH_2 fragment presently defined by the $H_{1,4}$ atoms.

Discussion of the Results

The protonation of a hydrocarbon with a large number of carbon atoms can take place at C−C or C−H bonds, to form the C-carbonium and H-carbonium cations via "three center−two electron" bonds. In an orbital scheme, the protonation over the C−H bond can be seen as the result of the overlap of the σ-orbital C−H with an s-orbital of the electrophilic hydrogen atom. In a similar way, in C−C protonated alkanes, the bonding is due to an overlap of two sp^3 orbitals belonging to adjacent carbon atoms and the 1s orbital of an atomic hydrogen. In the protonation of a CH_4 molecule, the situation is different with respect to other hydrocarbon and resembles the protonation of the NH_3 molecule (or other organic bases that contain heteroatoms) in which the protonation takes place at the heteroatom involving the lone pair electrons. Thus, the NH_3 molecule is protonated over the nitrogen lone pair. In the CH_4 molecule the protonation is carried out over the carbon atom and can be considered a three-centered bond formed by the overlapping of the σ-orbital of a hydrogen molecule with an empty sp^3 orbital of the carbon atom.

It must be pointed out that the topological analysis in species **1** and **2** indicates the existence of two BCPs at C−H* in the 3c−2e bond, contrary to what is usually found for higher carbonium ions, where a single BCP at the C−H* bond and a H*−H* bond is encountered.[36]

The missing bond critical point between the two H* atoms indicates that in these species there is formally no chemical bond between these two atoms, according to the Bader model. However, there are two bonds designated as C−H* (indicated by the existence of two bond critical points) with properties similar to each other. This situation allows us to state that the methonium ion—in species **1** and **2**—truly possesses a 3c−2e bond formed by H*−C−H* atoms, where three C−H bonds may be regarded as normal two-center−two-electron bonds and the bonding in the remaining CH_2 fragment is governed by the three-center−two-electron bond.

The inexistence of bond critical points between the two hydrogen atoms involved in the 3c−2e bonds would be the reason for the fluxionality of the CH_5^+ species (meaning that fluxional molecules are a subclass of *structurally nonrigid* molecules in which all the interconverting species that are observable are chemically and structurally equivalent). Since it is found that there is a bond critical point between the H* atoms for higher carbonium ions and a non-null activation barrier for bond-to-bond rearrangements in these species (making these rearrangements more difficult and leading to the nonfluxional structures), then it is interesting to imagine that the degree of fluxionality—the capability of a molecule to undergo fast and reversible intramolecular isomerization—and the existence of bond critical points between the H* should be related.

Actually, the nonexistence of a bond critical point between the H* atoms indicates that there is no effective bonding between them and this can be responsible for making the energy barriers for the bond-to-bond interconversion very small, since there is no H*−H* "bond" to break. This leads to a small differentiation among the several hydrogen atoms, leading to a highly fluxional species, as experimentally observed.

On the other hand, in the species **3** the four-center bond $C-H^*_{(2,3,5)}$ that is analyzed here is characterized by the presence of three BCPs that define three bond paths connecting the carbon atom with the three hydrogen atoms that lie in the same plane. The peculiar behavior of this electron-deficient species with multicenter σ-bonding, in which the bonding power of a pair of electrons is spread over more than two atoms, can be seen in the contour map of $\nabla^2\rho$. The analysis of the Laplacian values in the three BCPs and the contour map of $\nabla^2\rho$ in the plane that contains the carbon atom and the three hydrogen atoms mentioned above point toward the electronic delocalization in σ-bonds. Contrary to what happens in species **1** and **2**, the decrease in the parallel and perpendicular curvatures λ_2 and λ_3 of ρ is not so extreme and the variation in the absolute value of the relationship between both curvatures in these bonds is not so marked as those of the remaining bonds of the methonium

3 (i.e., $|\lambda_1/\lambda_3|$ between 1.57 and 1.65 in all the C−H bonds). This distribution of the electronic density and its Laplacian function, that in its contour map shows depletion regions of the concentration of the electronic density charge, reinforces the idea that this species would be stabilized, from the point of view of AIM, by the effect of the electronic delocalization in the $C-H^*_{(2,3,5)}$ fragment in which the bonding power of a pair of electrons is spread over the four atoms.

A study of the electronic delocalization of the interaction against four centers on the basis of delocalization indices is under development in our laboratory, and results will be presented elsewhere in the forthcoming future.

Conclusions

The topology of the distribution of the electronic density allows us to state that the methane molecule is protonated at the carbon atom, showing its pentacoordination clearly.

Thus, the carbon atom in the CH_5^+ ion is really directly bound to five hydrogen atoms. We have found and characterized five bond critical points between the carbon atom and the hydrogen atoms. The molecular graphs obtained for the different species of CH_5^+ agree with the proposed structures, with a carbon atom linked by bond paths to five hydrogen atoms.

In addition, it is interesting to highlight that this situation is unique among all the carbocations previously studied by our group.[36]

Beyond the hydrogen atoms in the methonium molecule, the zone behaves in a very fluxional way. The energy difference among species **1**, **2**, and **3** are very low, so that two different topological situations can be defined on the basis of the topology of the electronic charge density: species **1** and **2** present a bond H−C−H of 3c−2e type. However, in the species **3**, the absence of a 3c−2e bond deserves to be remarked. This structure can be characterized by the three BCPs found, corresponding to "saddle" points on the path bonds between the $C-H_{(2,3,5)}$ that lie in the same plane. The characteristic feature of the electron density in these electron-defficient species is the delocalization of the electron density, which is spread over the four nuclei localized in the same plane. It provides a further stabilization degree of the three C−H bonds involved in this interaction (the remaining two C−H bonds are similar to those of the nonprotonated species).

The 3c−2e bond existing in **1** and **2** species, denoted as H−C−H, presents different features as compared with the other 3c−2e bonds found in carbocationic species, where the 3c−2e bonds are established between two carbon atoms or carbon and hydrogen atoms and the central hydrogen atom (i.e., forming C−H−C and C−H−H bond types[36]). The four-center−four-electron bond encountered in species **3**, where the positive charge can be delocalized between the four centers, displays a singular contour map of the Laplacian of ρ in the plane containing these centers. The values of topological local properties at the three BCPs found in this species are indicative of σ-electron delocalization. The ellipticy values (diminished) and the electronic energy ($-E_b$) at BCPs show the stabilization of this species.

The idea of the existence of nonclassical bonds involving more than three centers cannot be completely excluded. Our results indicate that bonding situations with a higher number of atom arrays are possible in protonated hydrocarbon whenever the chemical system can be stabilized by electronic delocalization.

A study of the electronic delocalization, on the basis of the delocalization indices[41] in the context of AIM,[35] in the 4c−4e interaction proposed in this work is under development in our laboratory, and results will be published elsewhere soon.

Acknowledgment. The authors acknowledge the Supercomputer Center of the Secretary for the Technology, Science, and Productive Innovation, Argentine, for computational time. N.B.O. and N.M.P. thank the Facultad de Agroindustrias and SECYT UNNE for financial support. A.H.J. is a member of the Carrera del Investigador CIC. N.M.P. and N.B.O. are career researchers of CONICET, Argentina.

References and Notes

(1) Olah, G. A.; Rasul, G. *Acc. Chem. Res*. **1997**, *30*, 245.
(2) Thauer, R. K.; Klein, A. R.; Hartmann, G. C. *Chem. Rev.* **1996**, *96*, 3031 and references therein.
(3) Berkessel, A.; Thauer, R. K. *Angew. Chem.* **1995**, *107*, 2418; *Angew. Chem., Int. Ed. Engl*. **1995**, *34*, 2247.
(4) Car, R.; Parrinello M. *Phys. Rev. Lett*. **1985**, *55*, 2471.
(5) Corma, A. *Chem. Rev.* **1995**, *95*, 559.
(6) (a) Corma, A.; Miguel, P. J.; Orchilles, V. A. *J. Catal*. **1994**, *145*, 171. (b) Corma, A.; Planelles, J.; Sandoz-Marin, J.; Thomas, F. *J. Catal*. **1985**, *93*, 30. (c) Haag, W. O.; Dessau. R. M. In Proceedings 8th International Congress in Catalysis; DECHEMAL Frankfurt am Main, Berlin, 1984; Vol 2, p 305.
(7) (a) Olah, G. A. *Angew. Chem., Int. Ed. Engl.* **1973**, *12*, 173. (b) Olah, G. A.; Prakash, S. K.; Sommer, J. In *Superacids*; Wiley: New York, 1985.
(8) Olah, G. A.; Prakash, S. K.; Williams, R. E.; Field, L. D.; Wade, K. In *Hydrocarbon Chemistry*; Wiley-Interscience: New York, 1987.
(9) Olah, G. A.; Klopman, G.; Schlosberg, R. H. *J. Am. Chem. Soc.* **1969**, *91*, 3261.
(10) Tal'roze, V. L.; Lyubimova, A. K. *Dokl. Akad. Nauk. SSSR* **1952**, *86*, 909.
(11) Field, F. H.; Munson, M. S. B. *J. Am. Chem. Soc*. **1965**, *87*, 3289.
(12) French, M.; Kebarlé, P. *Can. J. Chem*. **1975**, *53*, 2268.
(13) Dyczmons, V.; Staemmler, V.; Kutzelnigg W. *Chem. Phys. Lett.* **1970**, *5*, 361.
(14) Müller, H.; Kutzelnigg, W.; Noga, J.; Klopper, W. *J. Chem. Phys*. **1997**, *106*, 1863.
(15) (a) Boo, D. W.; Lee, Y. T. *Chem. Phys. Lett*. **1993**, *211*, 358, (b) Boo, D. W.; Liu, Z. F.; Suits, A. G.; Tsé, J. S.; Lee, Y. T. *Science* **1995**, *269*, 57; Hiraoka, K.; Kebarle, P. *J. Am. Chem. Soc*. **1975**, *97*, 4179. Hiraoka, K.; Mori, T. *Chem. Phys. Lett*. **1989**, *161*, 111. Hiraoka, K.; Kudaka, I.; Yamabe, S. *Chem. Phys. Lett*. **1991**, *184*, 271. Heck, A. J. R.; de Koning, L. J.; Nibbering, N. M. M. *J. Am. Soc. Mass Spectrom.* **1991**, *2*, 453. Oka, T. *Philos. Trans. R. Soc. London Ser. A.* **1988**, *324*, 81.
(16) White, E. T.; Tang, J.; Oka, T. *Science* **1999**, *284*, 135.
(17) Schreiner, P. R.; Kim, S. J.; Schaeter, H. F.; Scheleyer, P. *J. Chem. Phys.* **1993**, *99*, 3716.
(18) Schreiner, P. R. *Angew. Chem., Int. Ed.* **2000**, *39*, 3239.
(19) Yeh, L. I.; Price, J. M.; Lee, Y. T. *J. Am. Chem. Soc.* **1989**, *111*, 5597.
(20) Hiraoka, K.; Kebarle, P. *J. Am. Chem. Soc*. **1976**, *98*, 6119.
(21) Asvany, O.; Kumar, P.; Redlich, B.; Hegemann, I.; Schlemmer, S.; Mark, D. *Science* **2005**, *309*, 1219.
(22) Huang, X.; McCoy, A. B.; Bowman, J. M.; Johnson, L. M.; Savage, C.; Dong, F.; Nesbitt, D. J. *Science* **2006**. *311*, 60.
(23) Jin, Z.; Braams, B. J.; Bowman, J. M. *J. Phys. Chem. A.* **2006**, *110*, 1569.
(24) Schleyer, P.; Carneiro, J. W. D. *J. Comput. Chem.* **1992**, *13* (8), 997.
(25) Collins, S. J.; O'Malley, P. *J. Chem. Phys. Lett.* **1994**, *228*, 246.
(26) Kolbuszewski, M.; Bunker, P. R. *J. Chem. Phys.* **1996**, *105*, 3469.
(27) Marx, D.; Parrinello, M. *Nature* **1995**, *375*, 216.
(28) Schreiner, P. R.; Kim, S.; Schaefer, H. F., III; Schleyer P. v. R. *J. Chem. Phys*. **1993**, *99*, 3716.
(29) (a) Marx, D.; Parrinello, M. *Science* **1999**, *284*, 59. (b) Marx, D.; Parrinello, M. *Z. Phys. D* **1997**, *41*, 253.
(30) Thompson, K. C.; Crittenden, D. L.; Jordan, M. J. T. *J. Am. Chem. Soc.* **2005**, *127*, 4954.
(31) Brown, A.; McCoy, A. B.; Braams, B. J.; Jin, Z.; Bowman, J. M. *J. Chem. Phys.* **2004**, *121*, 4105.
(32) McCoy, A. B.; Braams, B. J.; Brown, A.; Huang, X.; Jin, Z.; Bowman, J. M *J. Phys. Chem. A* **2004**, *108*, 4991.
(33) Brown, A.; Braams, B. J.; Christoffel, K.; Jin, Z.; Bowman, J. M. *J. Chem. Phys.* **2004**, *119*, 8790.
(34) Kumar, P and Marx, D., *Phys. Chem. Chem. Phys*. **2006**, *8*, 573.
(35) Bader, R. F. W. *Atoms in Molecules. A Quantum Theory*, Oxford Science Publications: Clarendon Press: London, 1990.

(36) (a) Okulik, N.; Peruchena, M.; Esteves, P. M.; Mota, C.; Jubert, A. H. *J. Phys. Chem. A.* **1999**, *103*, 8491. (b) Okulik, N.; Peruchena, M.; Esteves, P. M.; Mota, C.; Jubert, A. H. *J. Phys. Chem. A.* **2000**, *104*, 7586. (c) Okulik, N. B.; Esteves, P. M.; Mota, C.; Jubert, A. H.; Peruchena, N. M. *J. Phys. Chem. A.* **2002**, *106*, 1584.

(37) Marx, D.; Savin, A. *Angew. Chem., Ed. Engl.* **1997**, *36*, 2077.

(38) Tantillo, D. J.; Hoffmann, R. *J. Am. Chem. Soc.* **2003**, *125*, 4042.

(39) Frisch, M. J.; Trucks, G. W.; Schlegel, H. B.; Scuseria, G. E.; Robb, M. A.; Cheeseman, J. R.; Zakrzewski, V. G.; Montgomery, J. A., Jr.; Stratmann, R. E.; Burant, J. C.; Dapprich, S.; Millam, J. M.; Daniels, A. D.; Kudin, K. N.; Strain, M. C.; Farkas, O.; Tomasi, J.; Barone, V.; Cossi, M.; Cammi, R.; Mennucci, B.; Pomelli, C.; Adamo, C.; Clifford, S.; Ochterski, J.; Petersson, G. A.; Ayala, P. Y.; Cui, Q.; Morokuma, K.; Malick, D. K.; Rabuck, A. D.; Raghavachari, K.; Foresman, J. B.; Cioslowski, J.; Ortiz, J. V.; Baboul, A. G.; Stefanov, B. B.; Liu, G.; Liashenko, A.; Piskorz, P.; Komaromi, I.; Gomperts, R.; Martin, R. L.; Fox, D. J.; Keith, T.; Al-Laham, M. A.; Peng, C. Y.; Nanayakkara, A.; Gonzalez, C.; Challacombe, M.; Gill, P. M. W.; Johnson, B.; Chen, W.; Wong, M. W.; Andres, J. L.; Gonzalez, C.; Head-Gordon, M.; Replogle, E. S. and Pople, J. A. *Gaussian 98*, Revision A.7; Gaussian, Inc., Pittsburgh, PA, 1998.

(40) Blieger-Konig, W.; Bader, R. F. W.; Tag, T. H. *J. Comput. Chem.* **1982**, *3*, 317.

(41) Matta, C. F. AIMDELOC: Program to calculate the AIM electron localization and delocalization indices from the Fermi hole density. *QCPE* 0802, 2001.